

Molecular BioSystems

Accepted Manuscript



This is an *Accepted Manuscript*, which has been through the Royal Society of Chemistry peer review process and has been accepted for publication.

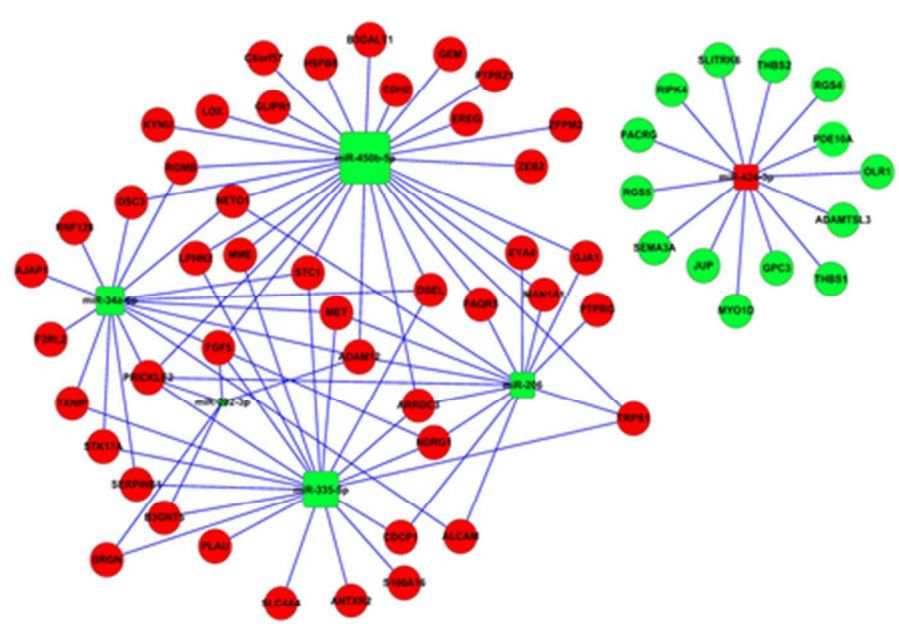
Accepted Manuscripts are published online shortly after acceptance, before technical editing, formatting and proof reading. Using this free service, authors can make their results available to the community, in citable form, before we publish the edited article. We will replace this *Accepted Manuscript* with the edited and formatted *Advance Article* as soon as it is available.

You can find more information about *Accepted Manuscripts* in the [Information for Authors](#).

Please note that technical editing may introduce minor changes to the text and/or graphics, which may alter content. The journal's standard [Terms & Conditions](#) and the [Ethical guidelines](#) still apply. In no event shall the Royal Society of Chemistry be held responsible for any errors or omissions in this *Accepted Manuscript* or any consequences arising from the use of any information it contains.



www.rsc.org/molecularbiosystems



Metastasis associated miRNA-gene-network in lung cancer

39x30mm (300 x 300 DPI)

Comprehensive gene and microRNA expression profiling reveals miR-206 inhibits MET in lung cancer metastasis

Qing-yong Chen^{a,1*}; De-min Jiao^{a,1}; Li Yan^{a,1}; Yu-quan Wu^a; Hui-zhen Hu^a; Jia Song^a; Jie Yan^a;
Li-jun Wu^a; Li-qun Xu^b; Jian-guo Shi^{b,*}

^aDepartment of Respiratory Disease, The 117th hospital of PLA, Hangzhou, Zhejiang, 310013, P.R. China

^bDepartment of Oncology Disease, The 117th hospital of PLA, Hang Zhou, Zhejiang, 310013, P.R. China

* Corresponding author 1: Qing-yong Chen. Tel.: +86 57187340861; fax: +86 57187340861.

E-mail: cqyong117@163.com

* Corresponding author 2: Jian-guo Shi. Tel.: +86 57187340801; fax: +86 57187340801.

E-mail: DrSJGuo@163.com

¹These authors contributed equally to this work.

Abstract

MiRNAs associated with the metastasis of lung cancer remains largely unexplored. In this study gene and miRNA expression profiling were performed to analyze the global expression of mRNAs and miRNAs in human high- and low- metastatic lung cancer cell strains. By developing an integrated bioinformatics analysis, six miRNAs (miR-424-3p, miR-450b-5p, miR-335-5p, miR-34a-5p, miR-302b-3p, miR-206) showed higher target gene degrees in the miRNA-gene-network and might be the potential metastasis related miRNAs. Using qRT-PCR method, the six miRNAs were further confirmed significant expression difference between human lung cancer and normal tissue samples. Since miR-206 was lower expression both in lung cancer tissues and cell lines, it was used as an example for further functional verification. Wound healing assay and transwell invasion assay showed that miR-206 mimics significantly inhibited cell migration and invasion of high-metastatic lung cancer 95D cell strain. One of its predicted targets in our miRNA-gene-network, MET, was also obviously decreased at protein level when miR-206 was overexpressed. Instead, miR-206 inhibitors increased MET protein expression, cell migration and invasion of low-metastatic lung cancer 95C cell strain. Meanwhile, luciferase assay showed that MET was direct target of miR-206. Furthermore, MET gene silence showed a similar anti-migration and anti-invasion effect with miR-206 mimics in 95D cells and could partially attenuated the migration- and invasion-promoting effect of miR-206 inhibitors in 95C cells, suggesting miR-206 targeting MET in the lung cancer metastasis. Finally, we also demonstrated that miR-206 can significantly inhibit lung cancer proliferation and metastasis in mouse models. In conclusion, our study provided a miRNA-gene regulatory network in lung cancer metastasis and further demonstrate the roles of miR-206 and MET in this process, which enhanced the understanding of regulatory mechanism in lung cancer metastasis.

Keywords: Lung cancer; Metastasis; Bioinformatics; Gene expression profile; miRNA expression profile; miR-206; MET

Introduction

Lung cancer, the leading cause of cancer deaths, has the most rapidly increasing incidence rate in the developed country ¹. Clinical data have showed that most lung cancer patients eventually suffered relapse and/or metastasis after complete excision of the cancer, even if they were at stage IA ². In addition, various analysis among a variety of cancers suggested that lung cancer has larger number of mutated genes than other cancers³. Therefore, the discovery of effective diagnostic markers and interrogating mechanisms of lung cancer development are both necessary for improving the survival rate of lung cancer patients.

MicroRNAs (miRNAs) are small noncoding RNAs that function as endogenous silencers of numerous target genes and have shown promises in both basic research and clinical application ⁴. Hundreds of human miRNAs have been identified in the human genome and some of them are crucially involved in cancer initiation and progression in that their expression profiles serve as phenotypic signatures of different cancers ^{5,6}. Given the urgent need to develop novel biomarkers or novel therapeutics for cancer, it is particularly promising to identify potential miRNA associated with the development, metastasis or suppression of cancer⁷. Increasing body of research has focused on the mechanisms underlying lung cancer metastasis, and differential expression of miRNAs also have been detected between lung cancer tissues and the adjacent normal tissues⁸. Gibbons et al demonstrated that forced expression of miR-200 abrogated the capacity of metastatic lung adenocarcinoma cells to undergo epithelial-to-mesenchymal transition, invade, and metastasize⁹. Tumor cell metastasis is regulated by miR-200 expression which is changed in response to contextual extracellular cues. Ma et al showed that silencing of miR-10b with antagomirs to mice bearing highly metastatic cells significantly increases the levels of Hoxd10 and markedly suppresses formation of lung metastases¹⁰. MiR-10b antagomir is well tolerated by normal animals and it appears to be a promising candidate for the development of new anti-metastasis agents. Other study demonstrated that miR-96 is significantly and consistently up-regulated in all 6 non-small cell lung cancers (NSCLCs)¹¹. They validated this result in an independent set of 35 paired tumors and their adjacent normal tissues, as well as their sera that are collected before surgical resection or chemotherapy, and the results suggested that miR-96 may play an important role in NSCLC development and has great potential to be used as a noninvasive

marker for diagnosing NSCLC. Although a few studies reported the aberrant expression and function of miRNAs in lung cancer, the identification of multiple miRNAs along with a comprehensive characterization of the miRNA/ mRNA interaction network may add a new level to our understanding of the gene regulation in lung cancer metastasis.

In the present study, we used gene and miRNA expression profiling to analyze the global expression of genes and miRNAs in human high- and low- metastatic lung cancer cell strains (strain 95D and strain 95C). By developing an integrated bioinformatics analysis of gene and miRNA expression profiling, we screened out six miRNAs (miR-424-3p, miR-450b-5p, miR-335-5p, miR-34a-5p, miR-302b-3p, miR-206) that were obviously different in expression between two strains, and have higher target gene degrees in our miRNA-gene-network. Specifically, miR-206 was lower expression both in lung cancer tissues and cell lines. Previous studies reported that miR-206 is downregulated in metastatic lung cancer¹², laryngeal cancer¹³, ovarian cancer¹⁴, rhabdomyosarcoma¹⁵. and its targets includes cyclinD2¹⁶, CDK4¹⁷, notch3¹⁸, MET¹⁹. MET controls growth, invasion and metastasis in cancer cells, including lung cancers^{20,21}. We now predicted that miR-206 targeting MET in lung cancer. Importantly, we performed further experiments *in vitro* and *in vivo* and confirmed the important roles of miR-206 and its target gene (MET) in lung cancer metastasis. Our findings suggest a previously unidentified molecular mechanism involved in the progression and metastasis of lung cancer.

Materials and methods

Cell lines and tissue samples

Human NSCLC cell strain, 95D (high-metastatic), 95C (low-metastatic)²², A549, 801D were purchased from the China Center for Type Culture Collection (CCTCC, China), and maintained in RPMI-1640 medium containing 10% fetal bovine serum (FBS, Gibco, USA), with 100 U/ml penicillin and 100 U/ml streptomycin. All the cells were grown in an atmosphere of 5% CO₂ at 37°C.

A total of 35 patients (20 adenocarcinoma patients, 15 squamous carcinoma patients) who were diagnosed as primary NSCLC in the Department of Respiratory Disease of The 117th Hospital of PLA from 2008 to 2012 were included in this study. None of these patients received

chemotherapy and radiotherapy before the surgery. Ethical approval was obtained from the hospital and fully informed consent from all patients before sample collection. Tumor and corresponding non-tumor lung tissue samples were collected and rapidly frozen in liquid nitrogen.

RNA extraction and quantification

Total RNA was extracted using Trizol reagent (Invitrogen, USA), according to the manufacturer's instructions. The quality and quantity of extracted RNA were assessed by spectrophotometry at A260/A280 on a Nanodrop ND-1000 Spectrophotometer and the denaturing agarose gel electrophoresis. The RNA samples were used for miRNA microarray and mRNA microarray experiments.

MiRNA array analysis

Our miRNA array analysis was based real-time quantitative PCR. Total RNA was isolated from cultured 95C, 95D cells. Reverse transcription was performed to generate the cDNAs. Samples were loaded onto preconfigured 384-well microfluidic cards (TaqMan Array Human MicroRNA A+B Card Set v3, Life Technologies) for real-time analysis of 774 human miRs (Sanger miRBase v18) using a 7900HT RT-PCR System (Life Technologies). Experimental data were then analyzed by SDS 2.2.2 software and the relative miRNA expression values were calculated using U6 snRNA as endogenous control according to the $\Delta\Delta C_t$ method²³. A Ct value less than 40 was defined as the limit of detection of the individual assays.

Gene microarray analysis

Total RNA was isolated from cultured 95C, 95D cells. A total of 100 ng of total RNA was reverse transcribed to cDNA. The biotinylated cDNA (5 μ g) was fragmented and hybridized to an Affymetrix GeneChip Human Gene 1.0 ST Array with 764,885 probes representing 28,869 genes. Genechips were then scanned using GeneChip Scanner 3000 7G Plus 2 and Command Console Software (AGCC) version 1.0 (Affymetrix Inc, Santa Clara, CA). Raw gene expression data in the generated CEL files were then normalized using the Robust MultiChip Averaging (RMA) algorithm²⁴.

Integrated analysis of different expression miRNAs and mRNAs

The relationships of differentially expressed miRNAs and mRNAs were further analyzed. The predicted miRNA targets were obtained using TargetScan version 5.1 and miRanda. Then, the intersection genes between the miRNA target genes and the different expression genes were screened out and analyzed by series test of cluster (STC) analysis.

Gene ontology (GO) analysis & pathway analysis

GO analysis was applied to analyze the main function of the screened differential expression genes according to the Gene Ontology which is the key functional classification of NCBI, which can organize genes into hierarchical categories and uncover the gene regulatory network on the basis of biological process and molecular function²⁵.

Pathway analysis was used to find out the significant pathway of the differential genes according to KEGG. Still, we turn to the Fisher's exact test and χ^2 test to select the significant pathway, and the threshold of significance was defined by $P < 0.05$ and (false discovery rate) $FDR < 0.1$.

MiRNA-gene-network

The microRNA-gene-network was based on the interactions of miRNAs and target genes²⁶. The significance of relationship of the miRNAs and target genes network was evaluated by the number of nodes in the network with degree greater than 15. Degree is the contribution of one miRNA to the genes around or the contribution of one gene to the miRNAs around. The key miRNA and gene in the network always have the higher degrees. In the miRNA-gene-network, the square represents miRNA and the circle represents gene, and their relationship was represented by one edge.

Plasmid constructs and transfection

To knockdown or overexpress miR-206, the cells were grown in complete medium for 24 h and then transfected with miRNA inhibitors or mimics (GenePharma, China), respectively. Assays were performed 24 h after transfection. MET gene was silenced using MET shRNA expression vector. 4 pairs of synthesized oligonucleotide inserts: sh-MET1, sh-MET2, sh-MET3 and sh-MET4 (Supplimentary table1) were annealed and cloned into the PGPU6/GFP/neo-shRNA expression vector (GenePharma, China) separately. Meanwhile, The plasmid PGPU6/GFP/neo-

shControl was used as the negative control (NC) and encoded a hairpin shRNA with a nonsense sequence. For stable cell line generation, the transfection was performed using Lipofectamine 2000 (Invitrogen) following the manufacturer's instructions. MET stable-knockdown cells and the control cells were selected using 0.3 mg/ml G418 (sigma).

Wound healing assay

Wound healing assay was conducted to examine the capacity of cell migration. Briefly, the wound was generated when the cells reached 90 - 95% confluent in 12-well plate by scratching the surface of the plates with a 10 μ l pipette tip. The cells were then incubated in 2.5% FBS for 24h, and then photographed using phase-contrast microscopy (Leica). The distance between the wound edges of the scratch area was analyzed using Adobe Photoshop 7.0. All experiments were performed in triplicate.

Cell invasion assay

The invasive potential of cells was measured in transwell insert with 8.0 μ m pore polycarbonate membrane (Corning) according to the manufacturer's instructions. The filter of top chamber was matrigel-coated with 50 μ l of diluted matrigel following the standard procedure and incubated at 37 $^{\circ}$ C for 2 h. The lower chambers were filled with 600 μ l of RPMI 1640 medium containing 10 % FBS as chemoattractant. Then 50,000 cells in 100 μ l serum-free medium was added into each top chamber. After the cells were incubated for 24 h, the non-invading cells that remained on the upper surface were removed with a cotton swab. The invasive cells on the lower surface of the membrane insert were fixed with cold methanol for 45 min, and then stained with 0.1% crystal violet for 30 min. The number of cells on the lower surface, which had invaded through the membrane, was counted under a light microscope in five random fields at a magnification of 100 \times . The experiments were repeated three times independently.

Western blot analysis

The whole-cell extracts were prepared in RIPA buffer (20 mM Tris, 2.5 mM EDTA, 1% Triton X-100, 1% deoxycholate, 0.1% SDS, 40 mM NaF, 10 mM Na₄P₂O₇ and 1 mM PMSF). Thirty micrograms cellular protein of each sample was applied to immunoblot following 10% SDS-PAGE electrophoresis and probed with indicated antibodies (MET antibody, Abcam

company), followed by a horseradish peroxidase-conjugated goat anti-mouse or anti-rabbit antibody (Millipore). Immunoreactive bands were visualized by enhanced chemiluminescence (Millipore) according to the manufacturer's instructions. Quantification of reactive protein bands was performed by densitometric analysis and the fold change was calculated by normalizing with control β -actin levels.

TaqMan miRNA real-time quantitative PCR analysis

Quantitative real-time PCR (qRT-PCR) was used to validate the miRNA expression results. The primers for RT-PCR to detect miRNA were designed based on the miRNA sequences provided by the Sanger Center miRNA Registry. The RT primers were designed as showed in supplementary materials (Supplimentary table 2). qRT-PCR was performed on the ABI (Applied Biosystems) 7900 HT Thermal cycler in standard mode for 40 cycles. Relative miRNA expression values (Target miRNA vs U6) were calculated with the $2^{-\Delta\Delta C_t}$ method²³. The data are representative of the means of three experiments.

Luciferase report assay

Luciferase reporter (pmirGLO vector, Promega) constructs containing portions (position:2030) of the c-met 3'-UTR (MET), mutant sequence (MET-mut) and miR-206 inhibitor sequence (Positive control, PC) were generated by GenePharma Inc (Shanghai, China). 95D and 95C cells were cultured in 24 well plates for 24 hours and cotransfected with 25 ng of c-met 3'-UTR reporter constructs and 20 nM of miR-206 mimics or mimic NC using lipofectamine 2000 for 24 hours. After transfection, cells were harvested, lysed, and assayed with the Dual-Luciferase Reporter Assay Kit (Promega) according to the manufacturer's instructions. Firefly luciferase activity was normalized to renilla luciferase activity for each transfected well. Each experiment was performed in duplicate and repeated three times.

Immunohistochemistry

Paraffin-embedded tissues (20 adenocarcinoma, 15 squamous carcinoma and 10 paratumorous tissues) were immunostained for MET protein as previously described²⁷. MET antibody was from Abcam company, 1:50 dilution.

***In vivo* assay**

All experimental procedures used in this study had been approved by the ethics committee in the 117th Hospital of PLA. Male nude mice (BALB/c, 4-6wk) were purchased from Shanghai Laboratory Animal Center (Shanghai, China). For preparation of subcutaneous xenograft model, 0.2 ml A549 lung cancer cells (2.0×10^6) in phosphate buffered saline/100 μ l were injected subcutaneously into the right flank of the nude mice. 15 days after tumor cell inoculation with confirmation of successful maturation of tumors, mice were divided randomly into two groups (five mice per group). They were treated with miR-206 agomirs or with miR-206 agomir negative control (NC) every three days for four weeks. miR-206 agomirs (2 nmol; Genepharma, Shanghai, China) were given locally by direct injection into the xenografts. The tumors were monitored with a caliper every six day and tumor volumes were determined (in cubic millimeter) by measuring in two directions and was calculated as tumor volume = length \times (width)²/2. Six days after the last injection of agomirs, all mice were killed according to the animal experimental guidelines. The xenografted tumors were excised and paraffin embedded for H&E staining.

Statistical analysis

All statistical analyses were performed using SPSS 13.0. Data were expressed as mean \pm SD. The Fisher exact test was used to examine possible correlations between the expression of miR-206 and clinicopathological factors. The statistical difference of data between groups was analyzed by one-way analysis of variance (ANOVA) and Student's t test. Differences were considered significant when $p < 0.05$.

Results

Identification and analysis of metastasis-related miRNAs and genes in human high and low-metastatic lung cancer cell strains

Strain 95D and 95C, isolated from poorly-different human large-cell lung carcinoma cell line PLA-801, were of different degrees of metastatic potential and tumorigenesis²². The invasive potential of two strains of cells was also confirmed in our lab. Analysis of both gene and miRNA expression is an important step towards understanding lung cancer metastasis. To identify

differential miRNA and gene expression between two strains, miRNA and mRNA microarray analysis were performed. miRNA microarray results were showed in Supplementary Table 3 (fold change >5 and $p < 0.05$ as a cutoff) and 14 miRNAs are found upregulated in strain 95D, while 16 miRNAs are downregulated. The miR-424-3p exhibited maximum upregulation (fold change 37.5) and the miR-202-3p exhibited maximum downregulation (fold change 591.2). Clustering analysis (MeV4.9.0 software) showed that these miRNAs falled into different clusters (Supplementary Figure.1). mRNA microarray analysis identified 96 up-regulated genes and 62 down-regulated genes in strain 95D using fold change > 2 and $p < 0.05$ as a cutoff (Supplementary table 4).

To better estimate the extent to which miRNAs regulate gene expression during lung cancer metastasis and identify target genes of differentially-expressed miRNAs in two strains of cells, integration analysis of gene and miRNA expression data were conducted. Among the 96 up-regulated genes in strain 95D , 68 are predicted targets of 16 downregulated miRNAs. Among the 62 down-regulated genes in strain 95D , 34 are predicted targets of 14 upregulated miRNAs. In order to investigate what functions the regulated genes may fulfill in lung cancer cells, we performed functional classification analysis of significantly-regulated genes using GO analysis and pathway analysis, and searched for significantly-enriched biological processes and pathways. Supplementary figure.2 and Supplementary figure.3 lists some top biological processes and pathways which were significantly-enriched in differentially-expressed genes between strain 95D and strain 95C. Genes that were downregulated in strain 95D were classified as related mainly to positive regulation of cell adhesion. Genes that were upregulated in strain 95D were classified as related mainly to blood vessel development. This result may reflect different level of cell adhesion and effect on angiogenesis between strain 95D and strain 95C. ECM-receptor interaction, TGF-beta signaling pathway, hematopoietic lineage and cell adhesion molecules ranked as the most significantly over-represented pathway among these genes, suggesting the importance of these pathways in lung cancer cell adhesion and angiogenesis. Interestingly, regulation of cell adhesion, motion and migration were over-represented among upregulated and downregulated genes in strain 95D, indicating that different metastasis-related genes were expressed between strain 95D and strain 95C.

Construction of miRNA-target gene regulatory network and screening of candidate miRNAs from the functional landscape of lung cancer metastasis

In order to discern the major candidate miRNAs associated with lung cancer metastasis, we used bioinformatics analysis to predict the most significant candidate miRNAs. The numbers of gene regulated by miRNA were represented by degrees. First, The miRNAs with degree > 15 and fold change > 10 were screened out (shown in Table1). GO and pathway significance analysis were used to screen the intersection genes and their functions. Then, based on the functions of miRNAs and their target genes, a regulatory miRNA-target gene network was constructed. As showed in Figure.1, The larger squares represent the more genes which are regulated. In total, both upregulated and downregulated miRNAs were identified to involve into the network. Among them, miR-424-3p was showed increased miRNA expression and miR-450b-5p, miR-335-5p, miR-34a-5p, miR-302b-3p, miR-206 were with reduced miRNA expression in strain 95D (compared with strain 95C). These six miRNAs were shown in the middle of network, regulating most of the selected target genes that related to lung cancer metastasis .

qRT-PCR detection of candidate miRNAs expression in human lung cancer cell lines and tissue samples

To verify the accuracy of microarray results and miRNA-target gene regulatory network, we measured expression of six candidate miRNAs in 5 cell samples (strain 95D, strain 95C, A549, 801D lung cancer cells and human normal lung bronchial epithelial BEAS-2B cells) and 45 paraffin-embedded tissue samples (20 adenocarcinoma, 15 squamous carcinoma and 10 para-tumorous tissues) by a real-time quantitative TaqMan qRT-PCR method. The results showed that Five miRNAs (miR-424-3p, miR-450b-5p, miR-34a-5p, miR-302b-3p, miR-206) have the similar expression trends between what was shown in microarray analysis and qRT-PCR analysis with only different magnitude of the fold changes in expression. One miRNA (miR-335-5p) was observed discordant between qRT-PCR and microarray results, which was found downregulated by microarray analysis but had no change ($P>0.05$) by qRT-PCR measurement. Among these miRNAs, miR-424-3p emerged as a slightly upregulated miRNA in a series of tested human lung cancer cell lines as compared with that found in normal lung epithelial cell and low-metastatic strain 95C cells. By contrast, miR-450b-5p, miR-335-5p, miR-302b-3p emerged as slightly

downregulated miRNA in high-metastatic strain 95D cells (data not shown). Consistent with the data obtained from lung cancer cell lines, the average expression level of miR-424-3p, miR-450b-5p, miR-335-5p, miR-302b-3p were also slightly higher or lower in the lung cancer tissue specimens than those in the non-tumour ones (Figure. 2). Only miR-206, emerged as highly downregulated miRNA, has a higher magnitude of fold changes both in high-metastatic strain 95D cells and lung cancer tissue specimens, which was used for further functional and mechanism study.

Correlation between miR-206 expression and clinicopathological features in NSCLC tissues

To further confirm that the expression level of miR-206 was associated with NSCLC metastasis, correlation analysis between the relative miR-206 expression levels and clinicopathological features of NSCLC was performed. The results were presented in Table 2. There was no correlation between the relative miR-206 expression levels and age and sex, but the relative miR-206 expression levels were significantly negatively correlated with tumor differentiation grade and regional lymph node involvement. The relative miR-206 expression level was significantly lower in patients with poorly differentiated NSCLC compared with patients with well and moderately differentiated NSCLC ($p < 0.05$) and in patients with lymph node involvement compared with patients without regional lymph node involvement ($p < 0.05$).

Anti-migration and invasion effects of miR-206 in lung cancer cell

It has been reported that expression of miR-206 is decreased in gastric cancer, breast cancer and lung cancer^{12, 28, 29}. Our bioinformatics analysis and qRT-PCR result further indicated that miR-206 may serve as a key molecular involved in high-metastatic potential of strain 95D. To verify the bioinformatics analysis results and the function of miR-206 in lung cancer metastasis, we transfected miR-206 mimics into strain 95D cells, which with low basal levels of miR-206. The results showed that overexpression of miR-206 significantly suppressed the migration and invasion of strain 95D (Figure.3a). Conversely, miR-206 inhibitor transfection increased strain 95C cell migration and invasion accordingly (Figure.3b), suggesting the negative regulation role of miR-206 in lung cancer cells migration and invasion.

miR-206 targeted MET in suppression of lung cancer cell migration and invasion

It has been reported that MET is closely associated with tumor invasion and metastasis^{30,31}. Based our target gene analysis and miRNA-target gene network, MET was showed one of targets of miR-206. To confirm the analysis results, we performed luciferase assays in lung cancer strain 95D and 95C cells. The results in Figure 4 suggested that miR-206 down-regulated the expression of MET by targeting its 3' UTR. In addition, we transfected miR-206 mimics and miR-206 inhibitors into strain 95D and strain 95C respectively, then MET protein expression was detected by western blot. The results were showed in Figure.5. Enforced expression of miR-206 triggered a silencing effect on the endogenous MET protein expression in strain 95D. Conversely, miR-206 inhibitors obviously increased the expression of MET in strain 95C cells. Interestingly, we found that specific shRNAs against MET could inhibit strain 95D cell migration and invasion (Figure.5a) and the inhibitory effects was similar to that of miR-206 mimics. To determine whether deregulation of MET is involved in regulation of cell migration and invasion by miR-206, we cotransfected strain 95C cells with miR-206 inhibitor and MET shRNA. The results showed that the migration- and invasion-promoting effects of miR-206 inhibitors were partially attenuated by MET shRNA (Figure.5b), suggesting that miR-206-induced suppression of lung cancer cell migration and invasion partly through inhibiting MET expression.

Correlation between miR-206 expression and MET expression levels in NSCLC tissues

To address the biological significance of the miR-206-MET interaction in NSCLC, immunohistochemistry (IHC) analysis was performed to detect the expression of MET protein in NSCLC and corresponding non-tumor lung tissues. Figure.6a displays representative images of the IHC staining for MET. In 10 cases of informative non-tumor lung tissues, negative (n = 8; 80%) or very weak (n = 2; 20%) cytoplasmic staining were detected. In contrast, all NSCLC tumor tissues showed positive immunostaining of MET protein: 15 of 35 NSCLC cases (42.85%) showed weakly positive and the remainder (57.15%) showed strongly positive. The correlation of MET overexpression with miR-206 expression levels in NSCLC tumor tissues was also studied, and results are summarized in Figure.6b. And apparently, overexpression of MET was significantly associated with lower miR-206 expression (P<0.01).

miR-206 inhibited lung cancer growth and metastasis *in vivo*

To investigate whether miR-206 is useful in inhibiting the growth and metastasis of lung cancer *in vivo*, we established A549 subcutaneous xenograft tumor model in nude mice. 15 days after inoculation, the mice were treated with miR-206 negative control (mimic NC) or miR-206 agomirs. The gross morphology of tumors and the results of final xenograft tumor weights measured on day 45 after tumor cell injection were showed in Figure.7a-b. Tumor wet weights were significantly lower in miR-206 agomirs treated tumors compared with miR-206-NC treated tumors (0.3765 ± 0.09628 versus 0.8879 ± 0.1345 , respectively; $P < 0.0001$; Figure.7b) Furthermore, the growth curves of xenografts (Figure.7c) showed that the tumors in the miR-206 agomirs group tended to grow more slowly than those in NC group. The volume of the tumors derived from the miR-206 agomirs treated group was dramatically reduced at 45 days compared to the negative control group. In addition, H&E staining showed that the tumors and tissues in miR-206 agomirs injected groups had clear boundaries with less invasiveness (Figure.7d). In contrast, tumors and lung tissues arising from control groups displayed characteristics of invasion. Taken together, these data indicated that the expression of miR-206 greatly inhibited the process of tumor progression *in vivo*.

Discussion

The malignant progression of a tumor from benign to invasive and metastatic is usually associated with a poor prognosis for cancer patients. Tumor metastasis is a highly complex and multistep process that includes altered cell adhesion, survival, proteolysis, migration, lymph/angiogenesis, immune escape, and homing on target organs. Cell motility and invasion are essential features of the metastatic process, and the identification and characterization of molecules and their associated pathways that control cell motility and invasion are critical to our understanding of cancer metastasis. High-metastatic strain 95D and low-metastatic strain 95C came from the same lung cancer cell line and have a similar genetic background, so they are ideal models for studying the mechanism of lung cancer metastasis. In order to enhance our understanding of lung cancer development and to explore the role of miRNAs during the lung cancer metastasis, we analyzed global gene and miRNA expression in these two strains. 14

up-regulated and 16 down-regulated miRNAs were identified. Bioinformatics analysis on differential expression genes showed cell adhesion, cell motion and cell migration are involved in mainly related biological processes. This observation may indirectly suggest that some of these genes are regulated at the protein level during lung cancer development and metastasis.

It has been shown that miRNAs accelerate the degradation of their target transcripts and repress their translation. Notably, mRNAs that were down-regulated and predicted to be targeted by up-regulated miRNAs also were enriched in mRNAs encoding proteins involved with lung tumor progression and metastasis in our gene and miRNA datasets. Two of these mRNAs was THBS1 and RGS5, which is down-regulated 6.4-fold and 5.8-fold respectively. Both these two genes are predicted to be targeted by miR-424-3p, which was up-regulated 37.5 fold. Since low THBS1 expression is associated with prognosis in advanced NSCLC³² and low expression of RGS5 is strongly associated with cancer vasculature invasion and lymph node metastasis in NSCLC³³, we speculate that the up-regulated miRNAs identified in this study may help dampen the expression of genes that act as a negative regulator of metastasis in NSCLC. Another example, the mRNA encoding the ADAM12 was up-regulated 2.14-fold in high metastatic cells and is predicted to be targeted by ten miRNAs that were down-regulated: miR-202-3p, miR-450b-5p, miR-34a-5p, miR-302b-3p, miR-29c-5p, miR-206, miR-200b-3p, miR-129-5p, miR-338-3p and miR-548d-5p. It is thus tempting to hypothesize that the down-regulated miRNAs identified in this study may act as progenitor maintenance factors helping to prevent aberrant or leaky expression of genes that would interfere with the tumor cells to acquire new adhesion and migration properties to emigrate from primary sites and colonize distant organs.

However, There were differentially regulated miRNAs identified in this study that did not have a negative correlation such as miR-99a-3p. It had a significant positive correlation with predicted target mRNAs. The lack of negative correlation could be caused by inaccuracies in miRNA target prediction or by a translational inhibition mechanism rather than RNA degradation, which would prevent detection with mRNA microarrays. The detection of miRNAs with a positive correlation between the miRNA and target mRNA (either both down-regulated or both being up-regulated) suggests some alternative indirect mechanisms or a positive regulatory role for miRNAs, as has been reported for some genes involved in cell migration. In view of the complexity of mRNA regulatory mechanism (mRNAs are most likely regulated by

additional mechanisms), we focused only on the miRNAs whose predicted target genes showed significant negative correlation to their cognate miRNA expression both in lung cancer cells and tissues.

Through integrating miRNA and mRNA expression profiling, a miRNA-mRNA negative regulatory network was constructed in our study. In this network, six miRNA classifying modules with higher target gene degrees and fold changes were screened out. Six modules' regulatory targets could be enriched in KEGG pathways, allowing an even clearer elucidation of their functional regulation patterns. We exemplified such analyses by looking at six miRNA modules whose target gene members were enriched in metastasis sub-groups, which might better imply the mechanisms of tumor progression and metastasis. Analysis results showed that miR-450b-5p targeted ZEB2, miR-335-5p targeted PLAU, miR-34a-5p targeted AJAP1, miR-206 targeted MET, miR-302b-3p targeted PTPRG and miR-424-3p targeted THBS2. Among these miRNAs and target genes, some have been well reported. For example, Yu et al reported that miRNA-34a suppresses proliferation and metastasis of human renal carcinoma cells by targeting CD44³⁴. Zhang et al reported that miRNA-34a suppresses cell migration and invasion of invasive urothelial bladder carcinoma by targeting Notch1³⁵. Yang et al reported that miRNA-34a suppresses breast cancer invasion and metastasis by directly targeting Fra-1³⁶. Peng et al reported that miRNA-34a inhibits the growth, invasion and metastasis of gastric cancer by targeting PDGFR and MET³⁷. Javeri et al reported that Downregulation of miR-34a is correlates with breast cancer metastasis³⁸, and so on. These findings suggest same miRNA may inhibit different cancer metastasis by targeting different genes. In this study, we predict miR-34a-5p targeted AJAP1 may be important in lung cancer metastasis. For miR-335-5p, it was reported that it can suppress invasion of lung cancer cell, neuroblastoma cell and osteosarcoma cells³⁹⁻⁴¹. In addition, THBS2 is reported associated with inhibition of supraglottic carcinoma and pancreatic cancer cell invasion^{42, 43}. These findings partly show the correctness of the our analysis results.

Some of the correspondences between the miRNAs and the target genes in our analysis have not been reported. Therefore, we choose one of miRNA-target pairs to further validate the miRNA-target gene relationships. MiR-206 was strongly and negatively related to its predicted target genes. We now predicted that miR-206 is involved in lung cancer metastasis by targeting MET, which may be an important and new viewpoint. To prove this, we performed further

experiments *in vitro* and *in vivo*. Luciferase report assay results proved that MET was a direct target of miR-206 in lung cancer 95D and 95C cells. Overexpression of miR-206 in strain 95D showed that it inhibits the protein expression of MET and lung cancer cell migration and invasion, which was similar to the results of MET gene silence. Further, miR-206 inhibitor treatment in low-metastatic strain 95C induced MET protein expression, cell migration and invasion, and the effects could be partially attenuated by MET shRNA. *In vivo*, we also found miR-206 can inhibit lung cancer growth and metastasis in subcutaneous tumor model in nude mice. These results suggest that miR-206 regulates MET in lung cancer and plays important roles in tumor progression and metastasis. MET is a receptor for hepatocyte growth factor (HGF), HGF/ MET axis is involved in multiple steps of metastasis^{44, 45}. We and others have found that MET protein was highly expressed in lung cancer tissues and related to more invasive and refractory properties⁴⁶. Thus, MET confers more invasive ability to strain 95D. Tight regulation of MET expression, therefore, appears essential during 95D cell migration and invasion. Regulation of MET by miR-206, which is suggested by our results, may further fine tune the MET protein to the necessary level. Both in high-metastatic cells and lung cancer tissues, where miR-206 is expressed at a relatively low level, it may cause high MET protein expression and further promote tumor progression and metastasis.

In our miRNA-target gene network, there are many other potential miR-206 targeted genes, like, NETO1, PAQR5, EYA4, MAN1A1, GJA1, and so on. Other researchers also reported that miR-206 functions as a tumor suppressor by targeting genes such as K-Ras⁴⁷, cyclinD2¹⁶, CDK4¹⁷, notch3¹⁸. Therefore, We have reasons to believe that miR-206 inhibited lung cancer metastasis not only by regulating MET. Furthermore, some of above predicted targets were found associated with lung cancer, miR-206 or adhesion. For example, EYA4 is reported associated with familial lung cancer risk⁴⁸. Cx43(GJA1) is reported up-regulation in TOF patients with miR-206 down regulated.⁴⁹ ADAM12 is reported often overexpressed in tumor cells and regulated cell adhesion/survival through MMP-14 and a PI3K/Akt signaling pathway⁵⁰. However, the roles of these targets in lung cancer metastasis need to be explored more in depth in our future studies.

Conclusions

In this study, the combined analysis of miRNA and mRNA expression profiles from lung

cancer cell strains with different metastatic potentiality provided a useful miRNA-target gene regulatory network related lung cancer metastasis, from which we predicted that miR-206 targeting MET, miR-450b-5p targeted ZEB2, miR-335-5p targeted PLAU, miR-34a-5p targeted AJAP1, miR-302b-3p targeted PTPRG and miR-424-3p targeted THBS2 in the lung cancer metastasis process. We took miR-206 as an example and demonstrated the roles of miR-206 and its target gene MET in the lung cancer cell migration and invasion. Meanwhile, we found that miR-206 can inhibit lung cancer growth and metastasis in mouse models with subcutaneous tumor xenografts. These results enhanced the understanding of molecular mechanism involved in lung cancer metastasis.

Acknowledgements

This work has been supported by '334' High-tech Talent Training Program of Nanjing Military Command, Public Welfare Project of Science and Technology Department of Zhejiang Province (2013C33209) and Science and Technology Plan Project of Hangzhou City (20130633B29).

Competing interests

The authors declare that they have no competing interests.

References

1. R. T. Greenlee, T. Murray, S. Bolden and P. A. Wingo, *CA: a cancer journal for clinicians*, 2000, **50**, 7-33.
2. J. C. Nesbitt, J. B. Putnam, Jr., G. L. Walsh, J. A. Roth and C. F. Mountain, *The Annals of thoracic surgery*, 1995, **60**, 466-472.
3. Z. Kan, B. S. Jaiswal, J. Stinson, V. Janakiraman, D. Bhatt, H. M. Stern, P. Yue, P. M. Haverty, R. Bourgon, J. Zheng, M. Moorhead, S. Chaudhuri, L. P. Tomsho, B. A. Peters, K. Pujara, S. Cordes, D. P. Davis, V. E. Carlton, W. Yuan, L. Li, W. Wang, C. Eigenbrot, J. S. Kaminker, D. A. Eberhard, P. Waring, S. C. Schuster, Z. Modrusan, Z. Zhang, D. Stokoe, F. J. de Sauvage, M. Faham and S. Seshagiri, *Nature*, 2010, **466**, 869-873.
4. N. Varol, E. Konac, O. S. Gurocak and S. Sozen, *Molecular biology reports*, 2011, **38**, 1079-1089.
5. M. I. Aslam, K. Taylor, J. H. Pringle and J. S. Jameson, *The British journal of surgery*, 2009, **96**, 702-710.
6. J. Manikandan, J. J. Aarthi, S. D. Kumar and P. N. Pushparaj, *Bioinformatics*, 2008, **2**, 330-334.
7. Z. Shan, Q. Lin, C. Deng, X. Li, W. Huang, H. Tan, Y. Fu, M. Yang and X. Y. Yu, *Molecular biology reports*, 2009, **36**, 1483-1489.

8. N. Yanaihara, N. Caplen, E. Bowman, M. Seike, K. Kumamoto, M. Yi, R. M. Stephens, A. Okamoto, J. Yokota, T. Tanaka, G. A. Calin, C. G. Liu, C. M. Croce and C. C. Harris, *Cancer cell*, 2006, **9**, 189-198.
9. D. L. Gibbons, W. Lin, C. J. Creighton, Z. H. Rizvi, P. A. Gregory, G. J. Goodall, N. Thilaganathan, L. Du, Y. Zhang, A. Pertsemliadis and J. M. Kurie, *Genes & development*, 2009, **23**, 2140-2151.
10. L. Ma, F. Reinhardt, E. Pan, J. Soutschek, B. Bhat, E. G. Marcusson, J. Teruya-Feldstein, G. W. Bell and R. A. Weinberg, *Nature biotechnology*, 2010, **28**, 341-347.
11. L. Ma, Y. Huang, W. Zhu, S. Zhou, J. Zhou, F. Zeng, X. Liu, Y. Zhang and J. Yu, *PLoS one*, 2011, **6**, e26502.
12. X. Wang, C. Ling, Y. Bai and J. Zhao, *Anat Rec (Hoboken)*, 2011, **294**, 88-92.
13. T. Zhang, M. Liu, C. Wang, C. Lin, Y. Sun and D. Jin, *Anticancer research*, 2011, **31**, 3859-3863.
14. S. Li, Y. Li, Z. Wen, F. Kong, X. Guan and W. Liu, *Molecular medicine reports*, 2014, **9**, 1703-1708.
15. R. Taulli, F. Bersani, V. Foglizzo, A. Linari, E. Vigna, M. Ladanyi, T. Tuschl and C. Ponzetto, *The Journal of clinical investigation*, 2009, **119**, 2366-2378.
16. J. Zhou, Y. Tian, J. Li, B. Lu, M. Sun, Y. Zou, R. Kong, Y. Luo, Y. Shi, K. Wang and G. Ji, *Biochemical and biophysical research communications*, 2013, **433**, 207-212.
17. R. W. Georgantas, 3rd, K. Streicher, X. Luo, L. Greenlees, W. Zhu, Z. Liu, P. Brohawn, C. Morehouse, B. W. Higgs, L. Richman, B. Jallal, Y. Yao and K. Ranade, *Pigment cell & melanoma research*, 2014, **27**, 275-286.
18. G. Song, Y. Zhang and L. Wang, *The Journal of biological chemistry*, 2009, **284**, 31921-31927.
19. D. Yan, E. Dong Xda, X. Chen, L. Wang, C. Lu, J. Wang, J. Qu and L. Tu, *The Journal of biological chemistry*, 2009, **284**, 29596-29604.
20. C. Birchmeier, W. Birchmeier, E. Gherardi and G. F. Vande Woude, *Nature reviews. Molecular cell biology*, 2003, **4**, 915-925.
21. P. C. Ma, R. Jagadeeswaran, S. Jagadeesh, M. S. Tretiakova, V. Nallasura, E. A. Fox, M. Hansen, E. Schaefer, K. Naoki, A. Lader, W. Richards, D. Sugarbaker, A. N. Husain, J. G. Christensen and R. Salgia, *Cancer research*, 2005, **65**, 1479-1488.
22. C. He, P. He, L. P. Liu and Y. S. Zhu, *Journal of cancer research and clinical oncology*, 2001, **127**, 180-186.
23. K. J. Livak and T. D. Schmittgen, *Methods*, 2001, **25**, 402-408.
24. R. A. Irizarry, B. Hobbs, F. Collin, Y. D. Beazer-Barclay, K. J. Antonellis, U. Scherf and T. P. Speed, *Biostatistics*, 2003, **4**, 249-264.
25. T. Schlitt, K. Palin, J. Rung, S. Dietmann, M. Lappe, E. Ukkonen and A. Brazma, *Genome research*, 2003, **13**, 2568-2576.
26. J. G. Joung, K. B. Hwang, J. W. Nam, S. J. Kim and B. T. Zhang, *Bioinformatics*, 2007, **23**, 1141-1147.
27. J. M. Wu, M. J. Fackler, M. K. Halushka, D. W. Molavi, M. E. Taylor, W. W. Teo, C. Griffin, J. Fetting, N. E. Davidson, A. M. De Marzo, J. L. Hicks, D. Chitale, M. Ladanyi, S. Sukumar and P. Argani, *Clinical cancer research : an official journal of the American Association for Cancer Research*, 2008, **14**, 1938-1946.
28. Y. Li, F. Hong and Z. Yu, *The Journal of international medical research*, 2013, **41**, 596-602.
29. Q. Yang, C. Zhang, B. Huang, H. Li, R. Zhang, Y. Huang and J. Wang, *European journal of gastroenterology & hepatology*, 2013, **25**, 953-957.

30. L. Trusolino, A. Bertotti and P. M. Comoglio, *Nature reviews. Molecular cell biology*, 2010, **11**, 834-848.
31. A. K. Mitra, K. Sawada, P. Tiwari, K. Mui, K. Gwin and E. Lengyel, *Oncogene*, 2011, **30**, 1566-1576.
32. T. Fleitas, V. Martinez-Sales, V. Vila, E. Reganon, D. Mesado, M. Martin, J. Gomez-Codina, J. Montalar and G. Reynes, *Clinical & translational oncology : official publication of the Federation of Spanish Oncology Societies and of the National Cancer Institute of Mexico*, 2013, **15**, 897-902.
33. G. Huang, H. Song, R. Wang, X. Han and L. Chen, *Journal of surgical oncology*, 2012, **105**, 420-424.
34. G. Yu, H. Li, J. Wang, K. Gumireddy, A. Li, W. Yao, K. Tang, W. Xiao, J. Hu, H. Xiao, B. Lang, Z. Ye, Q. Huang and H. Xu, *The Journal of urology*, 2014, **192**, 1229-1237.
35. C. Zhang, Z. Yao, M. Zhu, X. Ma, T. Shi, H. Li, B. Wang, J. Ouyang and X. Zhang, *Journal of Huazhong University of Science and Technology. Medical sciences = Hua zhong ke ji da xue xue bao. Yi xue Ying De wen ban = Huazhong keji daxue xuebao. Yixue Yingdewen ban*, 2012, **32**, 375-382.
36. S. Yang, Y. Li, J. Gao, T. Zhang, S. Li, A. Luo, H. Chen, F. Ding, X. Wang and Z. Liu, *Oncogene*, 2013, **32**, 4294-4303.
37. Y. Peng, J. J. Guo, Y. M. Liu and X. L. Wu, *Bioscience reports*, 2014, **34**.
38. A. Javeri, M. Ghaffarpour, M. F. Taha and M. Houshmand, *Med Oncol*, 2013, **30**, 413.
39. H. Wang, M. Li, R. Zhang, Y. Wang, W. Zang, Y. Ma, G. Zhao and G. Zhang, *Tumour biology : the journal of the International Society for Oncodevelopmental Biology and Medicine*, 2013, **34**, 3101-3109.
40. J. Lynch, J. Fay, M. Meehan, K. Bryan, K. M. Watters, D. M. Murphy and R. L. Stallings, *Carcinogenesis*, 2012, **33**, 976-985.
41. Y. Wang, W. Zhao and Q. Fu, *Molecular and cellular biochemistry*, 2013, **384**, 105-111.
42. W. Bai, L. Wang, W. Ji and H. Gao, *Acta oto-laryngologica*, 2009, **129**, 569-574.
43. B. Farrow, D. H. Berger and D. Rowley, *The Journal of surgical research*, 2009, **156**, 155-160.
44. C. R. Maroun and T. Rowlands, *Pharmacology & therapeutics*, 2014, **142**, 316-338.
45. J. L. Breindel, J. W. Haskins, E. P. Cowell, M. Zhao, D. X. Nguyen and D. F. Stern, *Cancer research*, 2013, **73**, 5053-5065.
46. L. Huang, S. J. An, Z. H. Chen, J. Su, H. H. Yan and Y. L. Wu, *Journal of thoracic oncology : official publication of the International Association for the Study of Lung Cancer*, 2014, **9**, 725-728.
47. F. Lin, L. Yao, J. Xiao, D. Liu and Z. Ni, *OncoTargets and therapy*, 2014, **7**, 1583-1591.
48. I. M. Wilson, E. A. Vucic, K. S. Enfield, K. L. Thu, Y. A. Zhang, R. Chari, W. W. Lockwood, N. Radulovich, D. T. Starczynowski, J. P. Banath, M. Zhang, A. Pusic, M. Fuller, K. M. Lonergan, D. Rowbotham, J. Yee, J. C. English, T. P. Buys, S. A. Selamat, I. A. Laird-Offringa, P. Liu, M. Anderson, M. You, M. S. Tsao, C. J. Brown, K. L. Bennewith, C. E. MacAulay, A. Karsan, A. F. Gazdar, S. Lam and W. L. Lam, *Oncogene*, 2014, **33**, 4464-4473.
49. Y. Wu, X. J. Ma, H. J. Wang, W. C. Li, L. Chen, D. Ma and G. Y. Huang, *World journal of pediatrics : WJP*, 2014, **10**, 138-144.
50. A. Leyme, K. Bourd-Boittin, D. Bonnier, A. Falconer, Y. Arlot-Bonnemains and N. Theret, *Molecular biology of the cell*, 2012, **23**, 3461-3472.

Figure legends

Figure.1: Candidate miRNAs-genes negative regulated network. The green square represent the down-regulated miRNAs, while the red circles indicate the up-regulated target genes in the 95D cells; The red square represent the up-regulated miRNA while the green circles indicate the down-regulated target genes in the 95D cells.

Figure. 2: Validation of microarray analysis data. The relative expression levels of six dysregulated miRNAs were determined by qRT-PCR. U6 was used as an internal control. Each qRT-PCR experiment was performed in triplicate. *P < 0.05, ** P < 0.01. Normal: non-tumor lung tissues.

Figure. 3: Ectopic miR-206 expression inhibits migration and invasion of lung cancer cells. 95D cells were transfected with miR-206 mimics, and 95C cells with miR-206 inhibitors. After transfection, wound healing assay and transwell invasion assay were performed to determine the ability of cell migration and invasion. Data represent the mean±s.d. The results were reproducible in three independent experiments. **P < 0.01 versus blank control group or indicated control.

Figure. 4: MET is a direct target of miR-206 in 95D and 95C cells. (a) 95D and (b) 95C cells were transfected with miR-206 mimics, followed by transfection with positive control reporter plasmids (PC) or MET mut 3' UTR plasmids (MET-mut) or MET3' UTR plasmids (MET) for 24 h. Reporter activity was measured with a luciferase assay and normalized to activity of Renilla luciferase. * P< 0.05, ** P< 0.01 compared with control.

Figure. 5: MET is involved in miR-206-induced suppression of lung cancer cell migration and invasion. miR-206 downregulated MET expression in lung cancer 95D cells and sh-MET1 significantly reduced the expression of MET protein and migration and invasion of 95D cells (a) Meanwhile, miR-206 inhibitors enhances MET expression in lung cancer 95C cells, and

cotransfected 95C cells with miR-206 inhibitor and sh-MET partially attenuated the migration- and invasion-promoting effects of miR-206 inhibitors (b). Data represent the mean±s.d. The results were reproducible in three independent experiments. *P < 0.05, **P < 0.01 versus blank control group or indicated control.

Figure. 6: Immunostaining of MET protein in primary NSCLC tissue samples. (a) Immunostaining of MET was negatively or very weakly positive in corresponding non-tumor lung tissues (I , II), but was weekly or strongly positive in lung adenocarcinoma (III, IV) and squamous cell carcinoma tissues (V ,VI). Original magnification,×100. Bar, 100 μm. (b)The immunoreactivity of MET protein in NSCLC tissues showed a statistically significant inverse correlation with the relative level of miR-206 expression. **P<0.01.

Figure. 7: miR-206 inhibited lung cancer growth and metastasis *in vivo*. (a) The comparison of tumor sizes in the miR-206 agomirs or NC groups after the xenografted tumors were excised. (b) the final xenograft tumor weights measured on day 45 after tumor cell injection. (*P < 0.05, **P < 0.01). (c) Tumor volumes of nude mice treated with miR-206 agomirs or NC. (*P < 0.05, **P < 0.01). (d) H&E staining showed that the tumors and tissues in miR-206 agomirs injected groups had clear boundaries with less invasiveness.

Table 1 The miRNAs with degree > 15 and fold change > 10

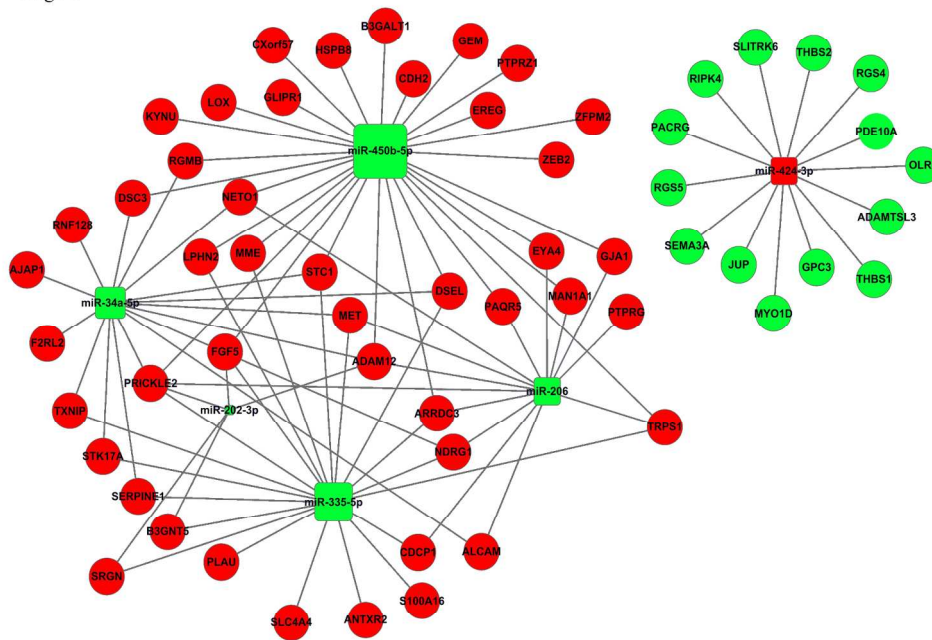
miRNAs	degree	fold change	regulation
miR-424-3p	16	37.473	up
miR-450b-5p	28	47.359	down
miR-302b-3p	23	16.338	down
miR-335-5p	20	32.518	down
miR-206	16	12.048	down
miR-34a-5p	16	32.205	down

Table 2 miR-206 expression and clinicopathological characteristics in NSCLC patients (n = 35)

Characteristics	No. of cases	miR-206 expression	<i>p</i>
Age (years)			
<60	12	28.76±0.77	0.78
≥60	23	28.64±1.38	
Gender			
Male	22	28.72±1.24	0.80
Female	13	28.61±1.14	
Histological subtype			
Squamous cell carcinoma	15	28.61±1.41	0.83
Adenocarcinoma	20	28.70±1.00	
Degree of differentiation			
Well and moderately	23	28.16±1.34	0.03*
Poorly	12	29.06±0.62	
Lymph node metastasis			
Negative	17	28.26±1.23	0.02*
Positive	18	29.11±0.77	
Tumor size			
<3cm	14	28.89±1.13	0.26
≥3cm	21	28.44±1.18	

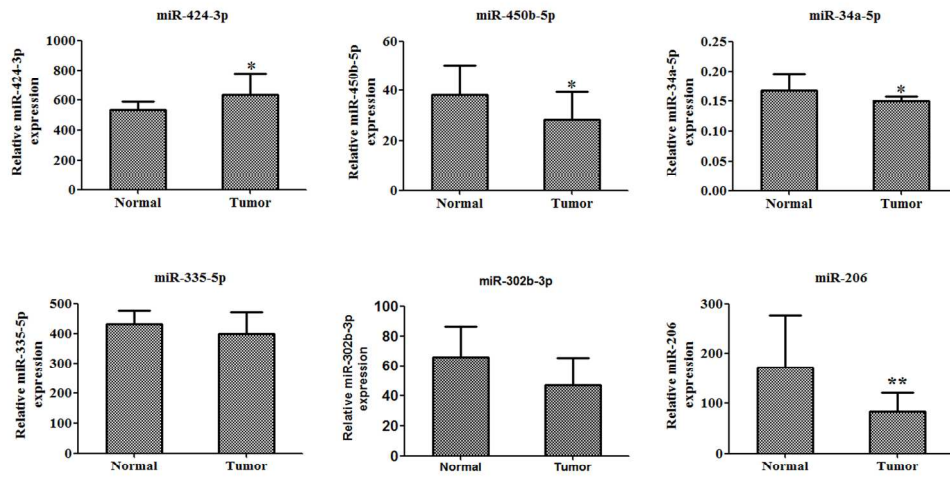
* Overall $p < 0.05$

Fig. 1



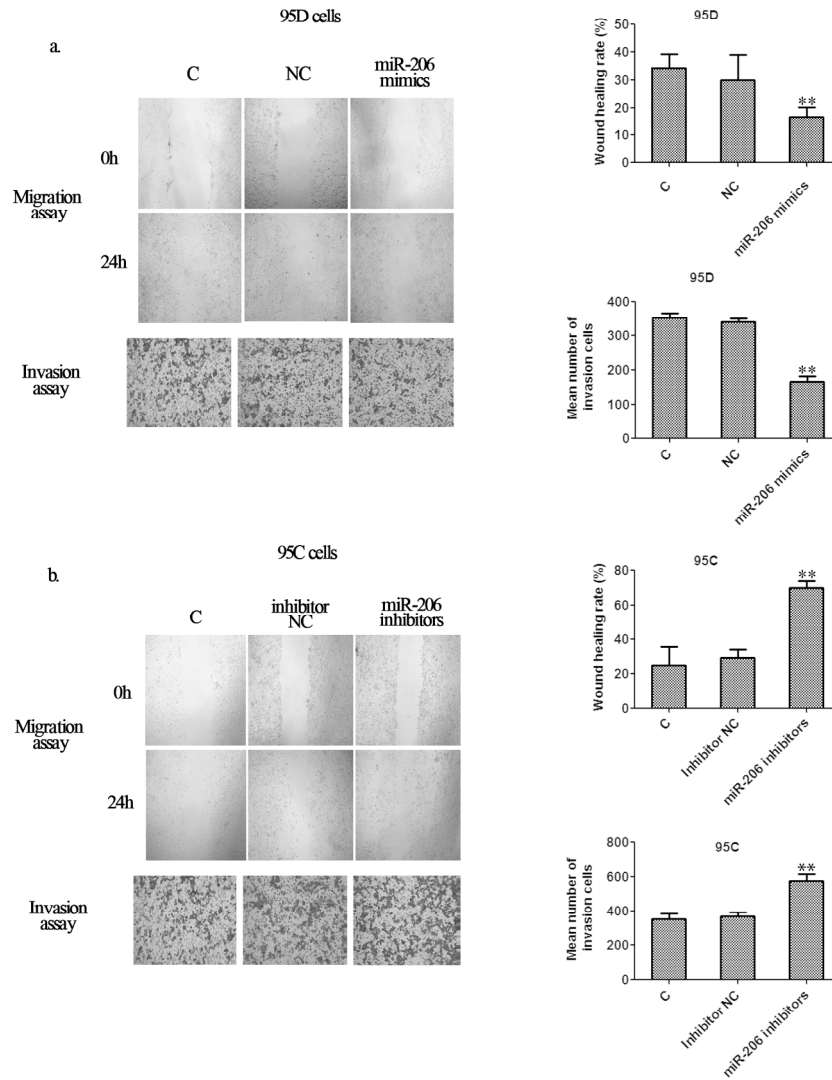
170x129mm (300 x 300 DPI)

Fig.2



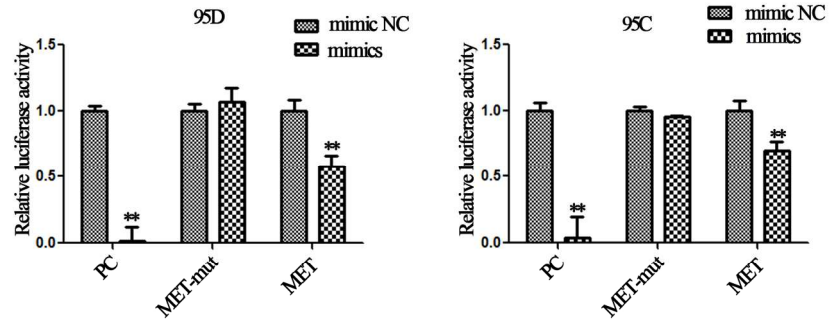
170x114mm (300 x 300 DPI)

Fig. 3



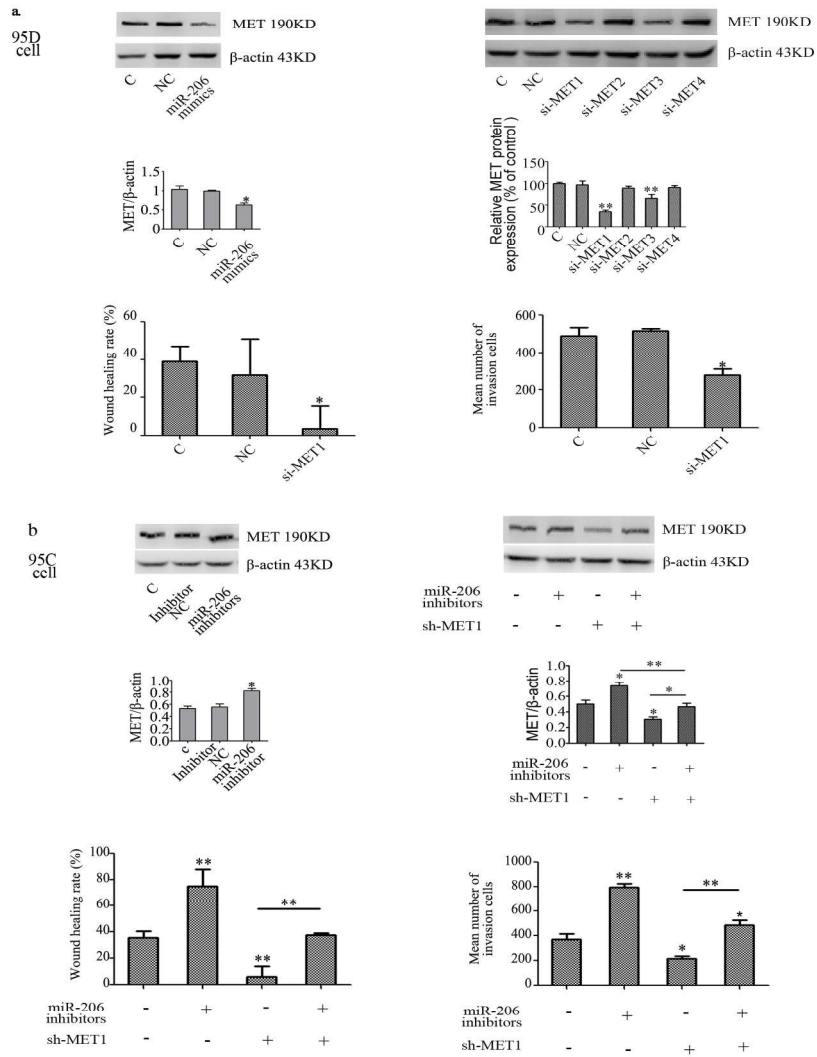
184x219mm (300 x 300 DPI)

Fig 4



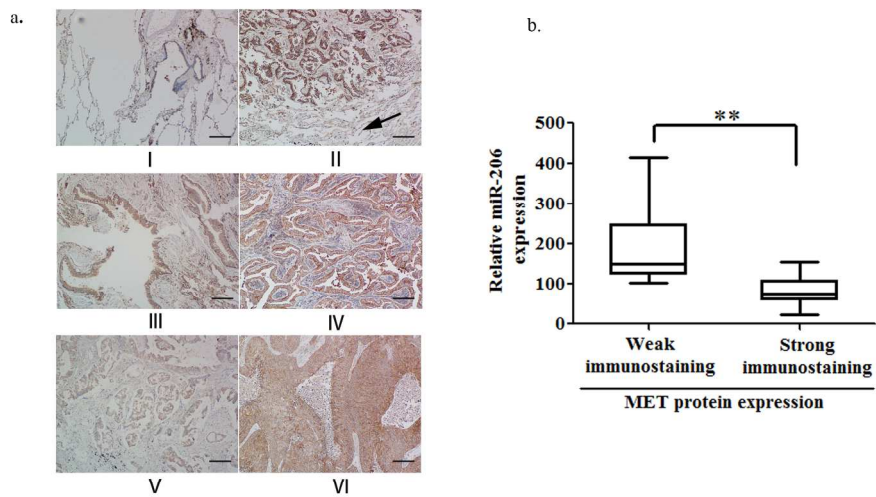
170x82mm (300 x 300 DPI)

Fig. 5



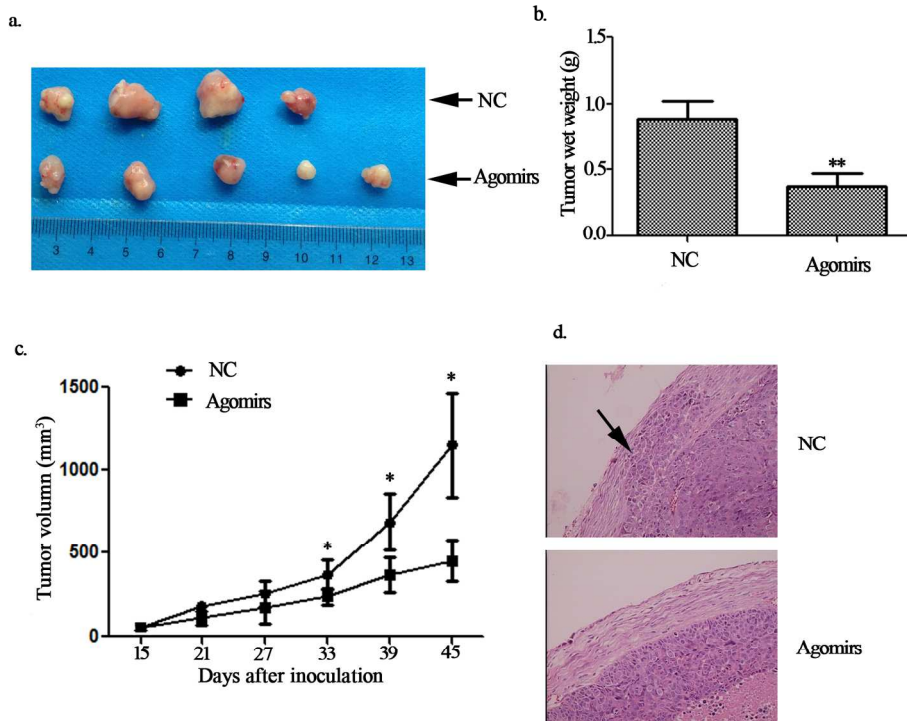
184x247mm (300 x 300 DPI)

Fig. 6



184x119mm (300 x 300 DPI)

Fig 7



170x160mm (300 x 300 DPI)